Characterized Microstructure and Electrical Properties of Hydrogenated Nanocrystalline Silicon Films by Raman and Electrical Conductivity Spectra

Gao Xiao-Yong[a,b,*], Zhao Jian-Tao[a], Liu Yu-Fen[a], Lin Qing-Geng[a], Chen Yong-Sheng[a], Gu Jin-Hua[a], Yang Shi-E[a] and Lu Jing-Xiao[a]

[a]The Key Lab of Materials Physics of Ministry of Education, Zhengzhou University 450052 Zhengzhou, China

[b]School of Physics and Engineering, Zhengzhou University, 450052 Zhengzhou, China

(Received October 1, 2008; in final form October 21, 2008)

Microstructure and electrical properties of hydrogenated nanocrystalline silicon (nc-Si:H) film deposited on glass substrate at low temperature were characterized by average grain size, crystallinity, and dark electrical conductivity data obtained from the Raman and electrical conductivity spectroscopy, respectively. The average grain size, crystallinity and electrical conductivity have a similar change with substrate temperature. A threshold substrate temperature determined by silane concentration appears in their corresponding spectroscopy vs. substrate temperature. The dependence of crystallinity, average grain size and electrical conductivity on substrate temperature were accounted for by surface diffusion model and heterojunction quantum dot model, respectively.

PACS numbers: 71.23.Cq, 73.61.−r

1. Introduction

More and more attention has been focused on hydrogenated nanocrystalline silicon (nc-Si:H) film because of its promising application to stable high efficiency solar cells [1–3], thin film transistors and panel display [4–6]. As a kind of candidate material, nc-Si:H has many special properties different from amorphous silicon such as higher electrical conductivity, smaller light-induced degradation and easy large-scale production. Its many applications for panel display, thin film resonance transistors and new optoelectrical sensor and detectors are based on its quantum size effects such as visible light photoluminescence [7] and tunneling effects [8]. On one hand, its microstructure determines its optoelectronic and electrical properties. On the other hand, silane concentration ((SC=$[SiH_4]/([SiH_4]+[H_2])$), substrate temperature (T_s) and other deposition parameters determine its microstructure. Generally, nc-Si:H is difficult to obtain due to the complex relationship between microstructure and deposition parameters. Based on it, its microstructure and electrical properties were characterized by average grain size, crystallinity and electrical conductivity data obtained from the Raman and electrical conductivity spectroscopy, respectively. The dependence of crystallinity, average grain size, and electrical conductivity on T_s were accounted for by surface diffusion model and heterojunction quantum dot (HQD) model, respectively.

* corresponding author; e-mail: xygao@zzu.edu.cn

2. Experimental details

A series of nc-Si:H films were deposited on glass substrate at different SC and T_s by using traditional radio frequency plasma-enhanced chemical vapor deposition (RF-PECVD) technique with an excitation frequency of 13.56 MHz. To avoid oxygen contamination, the base pressure in chamber is below 2×10^{-4} Pa and working pressure keeps a high value of 133 Pa which can effectively lower the damage to sample surface by the ion bombardment. The film microstructure was characterized by average grain size and crystallinity obtained from the Raman spectroscopy and electrical properties characterized by dark electrical conductivity. The film thickness was determined from reflectivity spectra in terms of interference effects. All the measurements above were done at room temperature.

3. Results and discussion

3.1 Mechanism of the film deposition

The deposition rate of as-deposited nc-Si:H films is shown in Fig. 1 as a function of SC. The result indicates that the deposition rate is nearly linear with SC, which can be accounted for by the following reversible reaction:

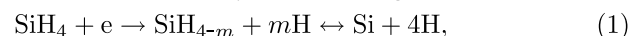

$$SiH_4 + e \rightarrow SiH_{4-m} + mH \leftrightarrow Si + 4H, \quad (1)$$

where m can be 1, 2, 3, which is determined by electron energy [9]. For the threshold energy of producing SiH_3, SiH_2, and SiH is 8.75, 9.47, and 10.33 eV [10], respectively, SiH_3 is the main precursor radical beside SiH_2 and SiH. SiH_4 reacts with plasma to produce active SiH_{4-m} and SiH_{4-m} decomposes into Si. This reaction is positive reaction. At the same time, H can destroy the weak Si–Si bonding and form active SiH_{4-m}, which is reverse

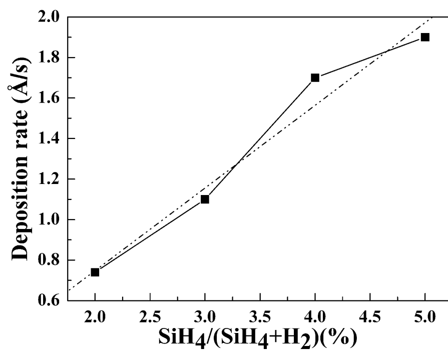

Fig. 1. Deposition rate of as-deposited nc-Si:H films as a function of silane concentration. The black squared and dash-dotted lines denote the measured and linear fitting line, respectively.

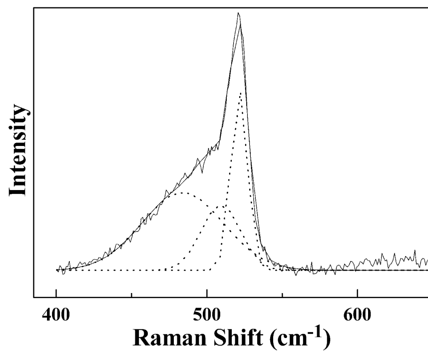

Fig. 2. Raman pattern for as-deposited nc-Si:H films.

reaction or called H-situ etch reaction. In terms of the reversible reaction (1), the larger SC helps to enhance the positive reaction and restrain the reverse reaction. Hence, the deposition rate is nearly in proportion to SC.

3.2 Characterization of the film microstructure

The crystallinity of nc-Si:H film is investigated by the Raman spectroscopy. By using the fitting method, the transverse optical phonon mode spectroscopy is decomposed into three peaks, a crystalline peak (520 cm^{-1}), an amorphous peak (480 cm^{-1}) and an intermediate peak (510 cm^{-1}). The Raman pattern of as-deposited nc-Si:H film is shown in Fig. 2. The dotted curves are the three-peak Gaussian fitting curves. The intermediate peak is considered to be due to grain boundaries, where increased bond lengths of the crystalline regions shift the Raman *peaks* to lower energy and to a grain size effect when the grain size is smaller than 15 nm [11]. The crystallinity for nc-Si:H can be described by formula 2 [12, 13]:

$$X_{\mathrm{c}} = (I_{510} + I_{520})/(I_{480} + I_{510} + I_{520}), \tag{2}$$

where I_{520}, I_{480}, and I_{510} are integrated intensities of the crystalline, amorphous and intermediate peak, respectively. The dependence of the crystallinity on T_{s} for nc-Si:H films is shown in Fig. 3. As can be seen from Fig. 3, the threshold T_{s} increases with SC increasing for SC smaller than 4%. Conversely, no threshold T_{s} is observed in Fig. 3 for the as-deposited film at 4% SC. It implies that the determined threshold T_{s} is higher by 400°C for 4% SC. The results can be explained by surface diffusion model [14]. From Fig. 1, the deposition rate is nearly linear with SC. Therefore, the larger SC leads to a larger deposition rate, which makes the main reaction precursor SiH_3 radical more difficult to migrate to lattice site by lattice relaxation method. On the other hand, the ratio of hydrogen coverage on film surface decreases with SC increasing. In terms of surface diffusion model, the main reaction precursor SiH_3 radical firstly migrates to a crystalline Si site on the hydrogen-terminated Si surface and then is stabilized by bonding two surface Si atoms after releasing one H atom in about 200 ps [15]. The smaller ratio of hydrogen coverage on film surface is, the more difficult SiH_3 radical is to diffuse to a crystalline site by migrating toward the smaller hydrogen coverage ratio surface [14]. To realize crystallization, SiH_3 radical has to migrate to crystalline Si site by the increase in kinetic energy resulting from the energy absorption from substrate surface. Hence, the larger SC is, the higher the threshold T_{s} of crystallization is. The crystallinity increases caused by the increasing kinetic energy and migration rate of SiH_3 radical with T_{s} increasing until the

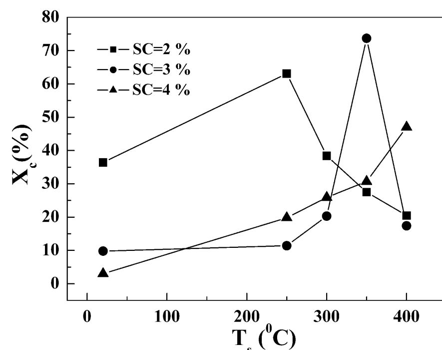

Fig. 3. Dependence of the crystallinity of as-deposited nc-Si:H films on substrate temperature.

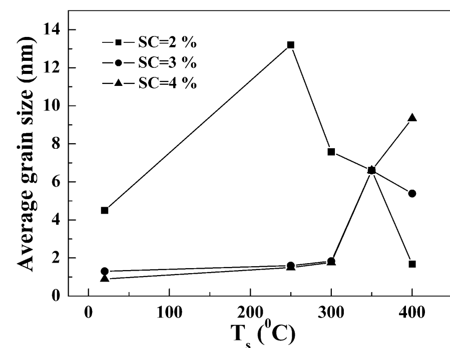

Fig. 4. Average grain size for as-deposited nc-Si:H films as a function of substrate temperature.

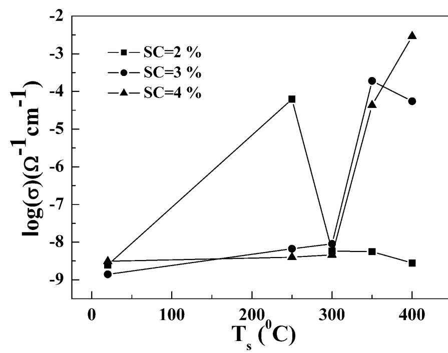

Fig. 5. Dark electrical conductivity of as-deposited nc--Si:H films as a function of substrate temperature.

threshold T_s. However, the crystallinity decreases due to the hydrogen releasing from surface and SiH_3 migration rate slowing down with T_s above the threshold T_s. The hydrogen releasing can distort the ordered Si net *and lowers* the crystallinity. *The average grain size d* for nc-Si:H film is shown in Fig. 4 as a function of T_s. It is calculated in terms of the following formula:

$$d = 2\pi(B/\omega)^{1/2}, \quad (3)$$

where the constant B is 2.21 nm^2/cm and ω is the deviation from the wave number of the standard crystalline silicon Raman peak. Figure 4 indicates a similar change between average grain size and crystallinity. It can also be explained by surface diffusion model. With T_s increasing, the main reaction precursor SiH_3 radical easily migrates to a crystalline Si site on the hydrogen-terminated Si surface and bonds two surface Si atoms by releasing one H atom. The stabilized Si grain size can become large due to the stack of Si atoms. However, when T_s is higher than the threshold T_s of crystallization, surface H atom can release from surface and distort the stabilized Si net, so the grain size can become *smaller*.

3.3 Characterization of the film conductivity

The dark electrical conductivity of as-deposited nc--Si:H samples is shown in Fig. 5 as a function of T_s. Figure 5 indicates that the electrical conductivity obviously changes in the range of 10^{-2} to 10^{-5} S/cm with T_s. The threshold T_s for electrical conductivity also appears in Fig. 5 implying a close relationship with crystallinity and average grain size. In terms of classical electrical theory, electrical conductivity is determined by free carrier concentration and mobility. However, as a kind of composite material made up of amorphous phase, grain boundary and nanocrystalline phase, the transport mechanism of nc-Si:H film is complex. In terms of heterojunction quantum dot model [16], nc-Si:H film is composed of alternating amorphous and microcrystalline regions, where the crystallinity keeps about 50%. Between amorphous and nanocrystalline regions, a grain boundary with 2–3 atom layer thickness exists. On the one hand, the nanocrystalline grains and their amorphous counterparts have very different band gap and band structures. As a result, they form heterojunction like structures in the interface regions. On the other hand, *nanocrystalline* grain acts like quantum dot. Free *carriers* can freely transport within grains, while transport to amorphous region *is exhibited* by quantum tunneling through the interface barrier. But the model may be modified. When the crystallinity of nc-Si:H films is far from 50%, only the area ratio of amorphous region to nanocrystalline region and grain boundary thickness are different from that obtained from HQD model. In such case, *as-deposited* nc-Si:H can also be treated in terms of HQD model. *Between nanocrystalline phase and amorphous phase a grain boundary barrier forms.* In terms of generalized Bayesian theorem (GBT) model used in polycrystalline silicon, the amount of acceptor surface *states* in the grain boundary *form* due to the surface absorption of oxygen and other gas atoms. Acceptor surface is electrically exhausted and charged to create a potential energy barrier, which impedes the transport of free *carriers* from one grain to another. For polycrystalline silicon, the conduction band near boundary is convex [17], while the density of acceptor surface state of nc-Si:H is one order smaller than that of polycrystalline silicon [18]. It is obviously attributed to the fill-up of the acceptor surface state by the existing hydrogen in the boundary of nc-Si:H [19]. Evangelistic once suggested that the discontinuity of valence band near grain boundary for crystalline Si/ amorphous Si (c-Si/a-Si) heterojunction can be neglected due to the disorder atoms at the grain boundary, while the conduction band near grain boundary is concave-downward [20]. Wang et al. also *discover* the concave-down conduction band near grain boundary of nc-Si:H film [21]. It is different from polycrystalline silicon. It may arise from the fill-up of acceptor surface state by donor hydrogen. In terms of HQD model, the band gap of nc-Si:H film is sketched in Fig. 6, where E_v, E_c, E_{cc} and E_i correspond to the valence band top, conduction band bottom for nc-Si:H, conduction band bottom for c-Si and interface level. In terms of classical semiconductor theory, the carrier concentration can be determined by the following formula:

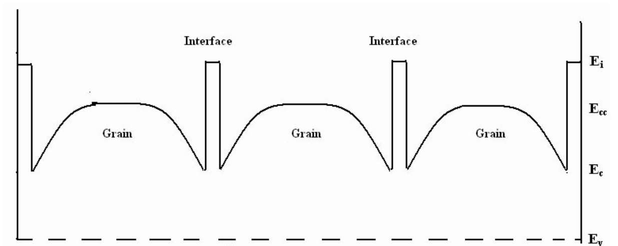

Fig. 6. Band sketch for nc-Si:H film in terms of HQD model.

$$n = n_0 \exp(-E_d/kT), \quad (4)$$

where E_d, n, and T are activation energy, free carrier concentration, and measurement temperature, respectively. For as-deposited nc-Si:H films, their E_d (about

0.4–0.5 eV) has a small difference, leading to a small difference between their free carrier concentrations at room temperature. According to classical semiconductor theory, dark electrical conductivity is described as follows:

$$\sigma = nq\mu, \tag{5}$$

where μ is the effective carrier mobility. The σ seemingly varies a little for different as-deposited nc-Si:H films. However, as indicated in Fig. 5, obvious *change* of electrical conductivity of films *takes* place in the range of 10^{-2} to 10^{-5} S/cm, implying the carrier concentration is not the main factor for electrical conductivity. Classical semiconductor theory is not appropriate for nc-Si:H films. A mandatory correction is required. The modified electrical conductivity of nc-Si:H can be described by the following formula [16] *in terms of* HQD model:

$$\sigma = ne\mu = \sigma_0 \exp(-E_d/kT)F(\langle q^2\rangle, T), \tag{6}$$

where E_d and $F(\langle q^2\rangle, T)$ are activation energy and quantum tunneling function, respectively. In terms with HQD model, free carrier can freely ballistically transport within grain, while transport to amorphous region is by quantum tunneling through interface barrier [16]. In terms of tunneling theory, the *small* interface thickness or interface barrier width helps the increase in quantum tunneling probability. In fact, the crystallinity *determines* the interface thickness. The larger crystallinity leads to the *smaller* interface thickness, which is the main reason for the increase *in* electrical conductivity with the crystallinity increasing. The free carrier concentration in amorphous regions is much smaller than in nanocrystalline region resulting from the quantum tunneling mechanism. On the other hand, the grain boundary can effectively diffract free carrier. Therefore, the effective carrier concentration can be greatly lowered due to the grain boundary and heterojunction between amorphous and nanocrystalline regions. The lowering effective carrier concentration can be regarded as the decreasing effective carrier mobility due to the carrier transport mechanism of nc-Si:H film. The effective carrier mobility rather than effective carrier concentration is the main effect factor for the dark electrical conductivity.

4. Conclusions

Microstructure and electrical properties of as--deposited nc-Si:H films on glass substrate at low temperature were characterized by average grain size, crystallinity and electrical conductivity data obtained from the Raman and electrical spectroscopy, respectively. The *results of our investigation* demonstrate that the deposition rate is nearly linear with SC, *which* can be explained by the reversible reaction in formula (1). The *average* grain size, crystallinity and electrical conductivity of the *nc-Si:H films* have a similar change with T_s. A threshold T_s determined by SC can be observed in their corresponding spectroscopy vs. T_s. The dependence of crystallinity, average grain size and electrical conductivity on T_s can be accounted for by surface diffusion model and heterojunction quantum dot model. The effective carrier mobility rather than free carrier concentration *has* the main effect on the dark electrical conductivity of as-deposited nc-Si:H films.

Acknowledgments

The work is supported by National Nature Science Foundation of China (grant No. 60807001) and National Basic Research Program of China (grant No. 2006CB202601).

References

[1] J. Meier, P. Torres, R. Platz, S. Dubail, U. Kroll, A.N. Selvan, N.P. Vauche, C. Hof, D. Fischer, A. Shar, K.D. Ufert, P. Giannoules, J. Koehler, *Mater. Res. Soc. Symp. Proc.* **420**, 3 (1996).

[2] K. Yamamoto, M. Yoshimi, T. Suzuki, Y. Tawada, T. Okamoto, A. Nakajima, *Mater. Res. Soc. Symp. Proc.* **507**, 131 (1998).

[3] K. Prasad, F. Finger, S. Dubail, A. Shah, M. Schubert, *J. Non-Cryst. Solids* **137**, 681 (1991).

[4] R. Galloni, *Renewable Energy* **8**, 400 (1996).

[5] C. Beneking, B. Rech, J. Foelsch, H. Wagner, *Phys. Status Solidi B* **194**, 41 (1996).

[6] H. Wagner, *Phys. Status Solidi B* **192**, 229 (1995).

[7] H. Takagi, H. Ogawa, Y. Yamazaki, A. Ishizaki, T. Nakagiri, *Appl. Phys. Lett.* **56**, 2379 (1990).

[8] E. Fortunato, R. Martins, I. Ferrira, M. Santos, A. Magarico, L. Guimaraes, *J. Non-Cryst. Solids* **115**, 120 (1989).

[9] T. Takagi, R. Hayashi, G. Ganguly, M. Kondo, A. Matsuda, *Thin Solid Films* **345**, 75 (1999).

[10] J. Perrin, O. Leroy, M.C. Bordage, *Contrib. Plasma Phys.* **36**, 3 (1996).

[11] S. Veprek, F.A. Sarott, Z. Iqbal, *Phys. Rev. B* **36**, 3344 (1987).

[12] M. Jana, D. Das, A.K. Barua, *Sol. Energy Mater. Sol. Cells* **74**, 407 (2002).

[13] T. Kaneko, K.T. Onisawa, M. Wakag, Y. Kita, T. Minemura, *Jpn. J. Appl. Phys.* **32**, 4907 (1993).

[14] M. Akihisa, *Thin Solid Films* **337**, 1 (1999).

[15] O. Tatusya, U. Osamu, N. Matsuhei, *Surf. Sci.* **458**, 216 (2000).

[16] Y.L. He, M.B. Yu, G.Y. Hu, Q. Zhang, *Acta Phys. Sinica* **46**, 1636 (1997).

[17] G. Harbeke, *Polycrystalline Semiconductors*, Springer-Verlag, New York 1985.

[18] Y.W. Seto, *J. Appl. Phys.* **46**, 5247 (1975).

[19] M.B. Yu, Y.L. He, H.T. Liu, J.S. Luo, *Acta Phys. Sinica* **44**, 634 (1995).

[20] F. Evangelistic, *J. Non-Cryst. Solids* **77-78**, 969 (1985).

[21] F. Wang, H.N. Lin, Y.L. He, A. Schweiger, R. Schwarz, *J. Non-Cryst. Solids* **137-138**, 511 (1991).